A Stochastic Spatio-Temporal Model of the Flow-Front Dynamics in a Vacuum Assisted Resin Transfer Moulding Process

Nauheimer, Michael; Relan, Rishi; Thygesen, Uffe Høgsbro; Madsen, Henrik; Olesen, Bendt; Kirkeby, Klaus

Published in:
I F A C Workshop Series

Link to article, DOI:
10.1016/j.ifacol.2018.09.175

Publication date:
2018

Document Version
Publisher's PDF, also known as Version of record

Available online at www.sciencedirect.com

ScienceDirect

IFAC PapersOnline CONFERENCE PAPER ARCHIVE

IFAC PapersOnLine 51-15 (2018) 383–388

A Stochastic Spatio-Temporal Model of the Flow-Front Dynamics in a Vacuum Assisted Resin Transfer Moulding Process

Michael Nauheimer * **Rishi Relan** ** **Uffe Høgsbro Thygesen** **
Henrik Madsen ** **Bendt Olesen** * **Klaus Kirkeby** *

* *Siemens Gamesa Renewable Energy, Denmark*
(e-mail: michael.nauheimer@siemens.com, bol@siemens.com, klaus.kirkeby@siemens.com)
** *DTU Compute, Technical University of Denmark, Denmark*
(e-mail: risre@dtu.dk, uhth@dtu.dk, hmad@dtu.dk)

Abstract: With more emphasis on the use of green energy, the size of the turbines and blades in the wind turbines is continuously increasing. With increasing blade size, the casting process becomes more complicated and the risk of faults increases. Production of such blades, made of fibre reinforced polymer composites, without the possibility of visual inspection of the infusion process calls for a sensor system (possibly virtual) for monitoring the process. Therefore, in this paper, we propose a stochastic spatio-temporal modelling approach to model the flow-front dynamics inside the vacuum assisted resin transfer moulding process, knowledge of which is essential for determining the current state of the infusion process.

Keywords: Wind turbines, Partial differential equations, Stochastic differential equations, Maximum Likelihood, Extended Kalman filter, Grey-box models

1. INTRODUCTION

Large scale composite shell structures like wind turbine blades consist of a glass fibre reinforced thermoset polymer structure. These structures are usually manufactured using the vacuum assisted resin transfer moulding (VARTM) process. The VARTM process involves infusing a thermoset polymer into a fibre reinforcement preform. Epoxy resin is transferred to the mould through several inlets. Progression of the epoxy inside the mould is only driven by the pressure difference between the mould and the pressure of one bar surrounding the mould in the production area.

Due to the inhomogeneous nature of the flow inside the mould, the risk of moulding defects such as dry spots and voids increases and this leads to deterioration of the mechanical properties of the cast parts (Sreekumar et al. (2007); Park et al. (2011); Matuzaki et al. (2015)). Hence, to prevent any potential fault from developing and for better control of the process, it is necessary to monitor the evolution of the flow-front inside the mould in a VARTM process.

Sensors for monitoring the VARTM processes is an active field of research. Several types of sensors have previously been implemented in VARTM processes including permittivity sensors (Yenilmez and Sozer (2009)), pressure sensors (Zhang et al. (2011)), and sensors based on electrical time-domain reflectometry (Dominauskas et al. (2003)). In general these sensors are accurate but limited to measuring on or close to the surface of the moulded parts. It has been shown in the past that sensors based on optical fibres (Kueh et al. (2002)) can be cast into parts making it possible to measure through thickness of the shell. Recently, (Matsuzaki and Shiota (2016)) proposed a method using two-sided visual observations for 4D data assimilation to accurately reconstruct the 3D resin flow and permeability filed of a fibre preform.

However, some blades produced at the *Siemens Gamesa Renewable Energy* factories are casted in one piece using the patented *IntegralBlades*® technology (Stiesdal et al. (2006)) instead of two separate half blades which are then united afterwards. One of the main disadvantages of this technology is that, it is not possible to visually inspect the process of transferring the epoxy resin to the mould. Hence, the main motivation at *Siemens Gamesa Renewable Energy* is to develop a flow-front monitoring system which eventually aids in controlling the process of mould filling. A controlled trajectory of the flow-front inside the mould decreases the risk of areas with dry glass, which eventually decreases the repair time and increase the general quality of the produced blade.

To achieve this goal, this paper proposes a spatio-temporal model to estimate the dynamics of the flow-front inside the mould. To emulate the real system, we first model the spatio-temporal evolution of the flow-front dynamics using partial differential equations (PDEs) based on Darcy's Law (Whitaker (1986)). The PDE based model is then simulated to generate different patterns of the evolution of the flow-front inside the mould.

⋆ We thank the *Manufacturing Academy of Denmark* (MADE) for providing the financial support. We thank the laboratory employees at *Siemens Gamesa Renewable Energy* for their assistance and suggestions.

10.1016/j.ifacol.2018.09.175

A PDE based model is generally not a preferred choice for online monitoring and control. Hence, the main contribution of this paper is to develop a spatio-temporal model of the flow-front dynamics using coupled stochastic differential equations (SDEs) (Øksendal (2010)). The validation of the coupled SDEs based model is performed for different patterns of flow-front dynamics generated using the PDE based model. Finally, an analysis of the level of measurement noise, sampling rate and the model complexity on the final estimated model is also presented.

The paper is structured as follows: Section 2 briefly describes the VARTM process. In Section 3, the mathematical background and implementation of PDEs based flow-front simulation model is discussed. A model for estimation of the flow-front based on coupled SDEs is proposed in Section 4. Section 5 describes the results and finally the conclusions are given in Section 6.

2. VARTM PROCESS

In this section, we briefly describe the VARTM process for blade manufacturing. Fig. 1 shows the work-flow of the VARTM process.

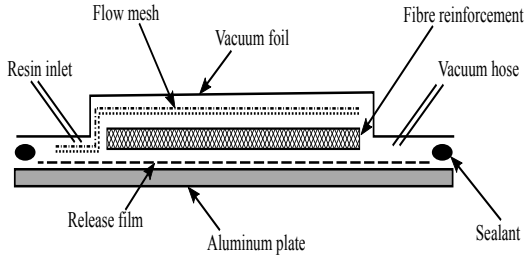

Fig. 1. The general material configuration and work-flow of a VARTM process. The resin enters the vacuum bag through the resin inlet and spreads into the pores of the fibre reinforcement from left to right. This process is only assisted by the vacuum generated through the vacuum hose.

The VARTM process is a special variety of Resin Transfer Moulding (RTM) processes. As the name indicates the process is only assisted by the difference of the near-vacuum inside the mould and the surrounding pressure of approximately one bar. The flow of epoxy inside the mould is dependent on e.g. the viscosity of the epoxy, the permeability, the porosity of the reinforcement materials and the pressure gradient.

Furthermore, the progression of the flow-front is highly dependent on both time and displacement of the front itself. This increases the challenge of estimating the flow-front. When epoxy is mixed it starts to cure immediately, increasing the viscosity over time. However, the continuous mixing of epoxy during the infusion of the mould decreases the cure rate. In addition, the viscosity of the epoxy is dependent on its temperature, with a higher temperature resulting in a lower viscosity but an increased cure rate. A decreased viscosity will result in an increased flow rate, but the epoxy curing process is an auto-catalytic exothermic process which will result in a fast increase of the temperature and thereby viscosity if heat cannot escape the blade mould.

3. SIMULATING FLOW IN A POROUS MEDIUM

To deal with the above mentioned challenges in practice, first it is important to completely understand the dynamics of the flow-front progression inside the mould. For that purpose, we first propose to simulate the flow-front progression in a VARTM process in a 80 cm × 90 cm rectangular casting for our simulation study. We have implemented Darcy's law with relevant boundary conditions into a PDE solver software, FEniCS Project (Alnæs et al. (2015)), and use the output to create flow-front pattern data representative of the data which can be measured experimentally using commercially available sensors and instrumentation (Nauheimer et al. (2017)). In the section below, we briefly explain the mathematical background behind the flow-front modelling.

3.1 Flow-front simulation model

Assumption 1: Epoxy is considered to be a Newtonian fluid.
Remark 1: Uncured epoxy is not a Newtonian fluid. It is assumed that minimal or equal distributed physical force will be exerted on the epoxy within the mould and thereby it is assumed that it can be considered a Newtonian fluid for our application.

Assumption 2: The increase in viscosity is small and constant enough to be omitted for shorter time scales.
Remark 2: The curing of epoxy initiates as soon as it has been mixed therefore, as the epoxy cures, the viscosity increases. It is assumed that for the short time frame of our simulations, the increase in viscosity is small enough to be omitted.

Assumption 3: A flow model described by Darcy's law in two spatial dimensions describes the general physics of a flow in three spatial dimensions.
Remark 3: With decreasing thickness of the preform, a three-dimensional formulation can be approximated well by the two-dimensional formulation.

The model of the flow-front propagation, can be formulated using PDEs determining the pressure as a function of space and time. We start with Darcy's law in two spatial dimensions

$$q = -\frac{\kappa H}{\mu}\nabla p \tag{1}$$

where $q = q(x, y, t)$ is the flow rate of the fluid, $\kappa = \kappa(x, y, t)$ is the permeability of the porous medium, H is a combined porosity and cross-sectional thickness measure, μ is the dynamic viscosity of the fluid, $p = p(x, y, t)$ is the pressure, and $\nabla = (\partial_x, \partial_y)$ is the spatial gradient. The flow rate is measured in m^2/s and is combined with the conservation of mass resulting in

$$\dot{h} + \nabla \cdot q = 0 \tag{2}$$

where $h = h(x, y, t) \leq H$ is the thickness of the fluid layer and $\dot{h}$ indicates time derivative of h. The density can be eliminated by assuming a relationship

$$h = \min(H, \frac{p}{\rho g}) \tag{3}$$

where ρ is the density of the fluid and g is the gravitational acceleration. Combining equations (2) and (3) results in,

$$\dot{h} = \frac{\mathrm{d}h}{\mathrm{d}p}\dot{p} = \nabla \cdot \left(\frac{\kappa H}{\mu} \nabla p \right) \tag{4}$$

This PDE is completed with boundary conditions: A pressure of zero at the outlet, a pressure of $p_0 = 1$ bar at the inlet, and no-flux boundary conditions along the sides. The PDE is then solved with FEniCS software (Alnæs et al. (2015)) numerically by time marching, using a semi-implicit Euler step where the derivative $\frac{\mathrm{d}h}{\mathrm{d}p}$ is evaluated at the previous time step, the time derivative $\dot{p}$ is approximated with a first order finite difference, and the right hand side is evaluated at the next time step. We note that $\frac{\mathrm{d}h}{\mathrm{d}p}$ vanishes in those parts of the domain that have already been filled with the fluid, so the system can be viewed as differential-algebraic. The numerical solution obtained from FEniCS is considered as our true data for this case study.

3.2 Simulated flow-front progression

The simulation model described above is used to emulate different flow-front patterns of the true system. The FEniCS software is configured such that the width is split into 64 cells and the length is split into 128 cells constructing a mesh of 64 × 128 cells and creating a total number of 65 × 129 vertices. The chosen amount of cells creates the opportunity for including a large number of lines to measure along, when trying to estimate a flow model and trying to determine the flow-front progression.

Assumption 4: Epoxy enters the mould evenly across a line perpendicular to the flow direction.
Remark 4: The epoxy can only enter the mould through one or several inlet points. In an experimental setup a cavity can be created to ensure a homogeneous inlet across a line perpendicular to the flow direction.

While specifying the placement of glass fibre and auxiliary materials in a blade mould, it is ensured that the evolution of the flow-front during infusion process is homogeneous. However, sometimes due to manufacturing errors materials are handled and placed less carefully than specified, resulting in perturbations in the flow-front progression during the infusion process. Therefore, here both a homogeneous case, where the value of $\frac{\kappa}{\mu}$ is kept constant with respect to (w.r.t) time and displacement, and a heterogeneous case are simulated. In the heterogeneous case $\frac{\kappa}{\mu}$ is kept constant only w.r.t the time but along the spatial directions we choose to model it as

$$\frac{\kappa}{\mu} = \frac{c_0}{\left(1 - A \cdot \cos\left(\frac{2\pi x}{L_x}\right)\right)\left(1 - A \cdot \cos\left(\frac{2\pi y}{L_y}\right)\right)} \tag{5}$$

where A is a constant determining the relative decrease in permeability towards the middle, c_0 being a correction constant and $L_x = 0.8$ m ; $L_y = 0.9$ m are the width and length of the casted area. This model describes a decrease of the permeability towards the centre of the cast area.

Fig. 2 shows a homogeneous flow-front progression with measurement noise added. The points are measurements at different, equally spaced, time steps along the y-axis where the preform is fully covered with epoxy. It is seen that the flow-front moves ahead evenly across the entire width of the preform. The time steps are evenly spaced showing that the velocity decreases with the progression

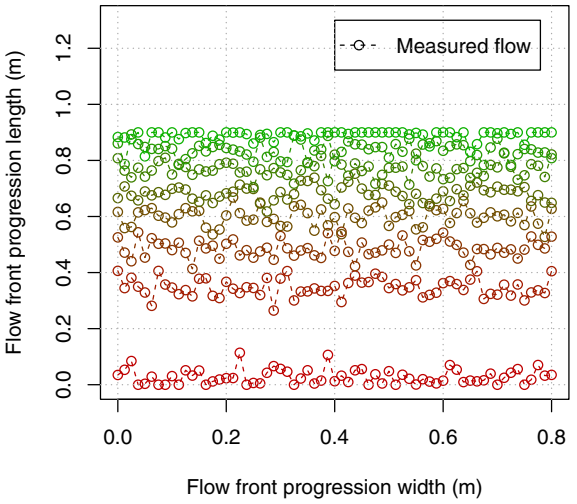

Fig. 2. Simulated output data of a homogeneous flow-front from FEniCS with added measurement noise. The line colour changes gradually from red at the first time instance to green at the last time instance as the flow-front evolves with time. All time steps are equal.

of the flow-front. Fig. 3 shows a heterogeneous flow-front

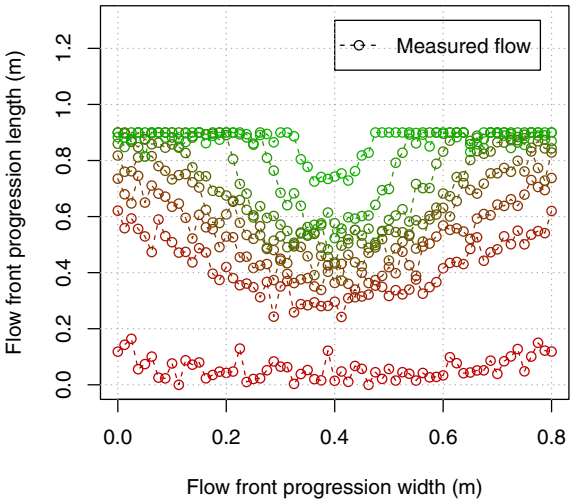

Fig. 3. Simulated output data of a heterogeneous flow from FEniCS with added measurement noise. The line colour changes gradually from red at the first time instance to green at the last time instance as the flow-front evolves with time. All time steps are equal.

progression with added measurement noise. In Fig. 3 it is seen how the decrease in the permeability also causes decreased flow rate towards the middle when comparing to the homogeneous flow shown in Fig. 2.

From the discussion above it is seen that the dynamics of the flow-front can be formulated as spatio-temporal model describing the pressure as a function of time and space. This formulation is very useful to simulate the propagation of the flow-front inside the mould for different scenarios and operating conditions (e.g. permeability, temperature etc.) as demonstrated.

Although these high-dimensional PDEs based models are good to understand and simulate a dynamical process they are not very useful when the final intended purpose of the

model is control and monitoring. Hence in the next section, we propose to use a coupled stochastic differential equation (SDE) (Øksendal (2010)) based modelling approach to model the flow-front dynamics.

4. LUMPED APPROXIMATION

In this section, we introduce first briefly the concept of SDE and thereafter we show, how the coupled SDEs can be used to approximate the flow-front dynamics inside the mould along the spatial directions.

4.1 Stochastic Differential Equations and Grey-box Models

Grey-box models are typically SDEs based models (Kristensen et al. (2004)), where the structure of the model is built based on a combination of physical knowledge of the system, as in the white-box models, and on the statistical information based on the observations (measured data), as in the case of the black-box models. From a theoretical point of view, SDEs are the preferred choice to model stochastic, complex, and nonlinear systems where only a partial information about the system dynamics is available. An SDE based state-space model can be written as:

$$\mathrm{d}Y_t = f(Y_t, U_t, t, \theta)\mathrm{d}t + \sigma(U_t, t, \theta)\mathrm{d}w_t \tag{6}$$
$$Z_k = h(Y_k, U_k, t_k, \theta) + e_k \tag{7}$$

The equations describing the dynamics of the states of the system, Y_t, are formulated in continuous time and are separated in a drift term, $f(Y_t, U_t, t, \theta)$, and a diffusion term, $\sigma(U_t, t, \theta)$. The observations, Z_k, are linked to the states through the observation equation (7), which are typically formulated in discrete time and include the measurement error, e_k. U_t represents the inputs and θ the parameters of the system.

A clear separation of the residual error into diffusion and measurement noise results in a more correct description of the prediction error (Øksendal (2010)). Inclusion of the diffusion has another advantage, mainly related to the model building itself. By investigating the diffusion terms, one can retrieve information about how to improve an insufficient model (Kristensen et al. (2004)). Diffusion terms that are estimated to be relatively large indicate a model mismatch for the relevant part of the model. SDEs have been found to be useful within many areas of mathematical modelling of many dynamical systems (Øksendal (2010)).

4.2 Discretisation of the Spatial Domain

The PDE model developed in the previous section is too complex for online monitoring and control purpose. Hence, we propose to use the coupled SDEs to model the flow-front dynamics for a limited amount of spatial discretisation points (as shown in Fig. 4) as compared to the PDE based model. First, note that one solution to the PDE in the homogeneous case, and for small H, is:

$$p(x, y, t) = p_0 \cdot \max(0, 1 - \frac{y}{Y_t}), \tag{8}$$

where Y_t is the position of the front, given by:

$$\frac{\mathrm{d}Y_t}{\mathrm{d}t} = \frac{\kappa p_0}{\mu}\frac{1}{Y_t}, \tag{9}$$

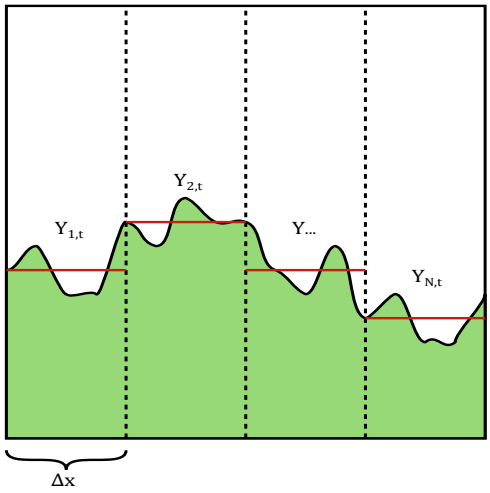

Fig. 4. A pictorial representation, how the flow-front is approximated using the coupled SDEs. The red line shows the domain of spatial dimension x which is approximated using a SDE, whereas the dotted vertical lines show the points of discretisation for the spatial dimension x.

and the material is flowing in the direction of the y-axis throughout the domain. Based on this, we discretise the x-axis using N grid points, and let $Y_{i,t}$ denote the position of the front at the corresponding value of x. No coupling between neighbouring grid points, results in N ordinary differential equations:

$$\frac{\mathrm{d}Y_{i,t}}{\mathrm{d}t} = \frac{\kappa p_0}{\mu}\frac{1}{Y_{i,t}}, \tag{10}$$

Since these equations assume perfect homogeneity, we introduce a noise term $\sigma_{i,t}$ which parameterises all conceivable differences between the model and the true system. Finally, if the front is not perfectly aligned with the x-axis, the material flow will neither be perfectly aligned with the y-axis. This will stabilise the shape of the front, and this effect is included in the model through a diffusive term:

$$\mathrm{d}Y_{i,t} = \left(\frac{\kappa p_0}{\mu}\frac{1}{Y_{i,t}} + D\frac{Y_{i+1,t} - 2Y_{i,t} + Y_{i-1,t}}{(\Delta x)^2}\right)\mathrm{d}t + \sigma_{i,t}\mathrm{d}w_t \tag{11}$$

For $i = 2, \ldots, N-1$, with similar equations for $i = 1, N$. For the actual estimation of a model, we choose a model where $\frac{\kappa p_0}{\mu}$ is combined to a single constant for each state equation, $c_{0,i}$, and $\frac{D}{(\Delta x)^2}$ is treated as a single global constant, D_0, for all state equations. This results in the following model being implemented

$$\mathrm{d}Y_{i,t} = \left(\frac{c_{0,i}}{Y_{i,t}} + D_0 \cdot (Y_{i+1,t} - 2Y_{i,t} + Y_{i-1,t})\right)\mathrm{d}t + \sigma_{i,t}\mathrm{d}w_t \tag{12}$$

Except for the boundary cases where we model it as

$$\mathrm{d}Y_{1,t} = \left(\frac{c_{0,1}}{Y_{1,t}} + D_0 \cdot (Y_{2,t} - Y_{1,t})\right)\mathrm{d}t + \sigma_{1,t}\mathrm{d}w_t \tag{13}$$

We argue that these equations, while a stretch from the original physics, capture the essential dynamics of flow-front propagation and are in a form suitable for online flow-front estimation.

4.3 Maximum Likelihood Estimation of SDEs

The parameters, $c_{0,i}$ and D_0, of the coupled SDEs formulated above to model the evolution of the flow-front dynamics are estimated from the measured data simulated using the complex PDE based model. Because of the complex structure of SDEs, estimation of parameters is non-trivial except for some simple cases. Hence we propose to use a maximum likelihood method in combination with an extended Kalman filter method described in (Kristensen et al. (2004)) to estimate the parameters. The likelihood function is formulated using the one-step prediction errors, ϵ_k, and the associated variances, $R_{k|k-1}$:

$$L(\theta; \mathcal{Z}_\mathcal{N}) = p(\mathcal{Z}_\mathcal{N}|\theta) \tag{14}$$
$$= \left(\prod_{k=1}^{\mathcal{N}} \frac{\exp\left(-\frac{1}{2}\epsilon_k^T R_{k|k-1}^{-1} \epsilon_k \right)}{\sqrt{\det(R_{k|k-1})(\sqrt{2\pi})^\mathcal{L}}} \right) p(z_0|\theta)$$

where θ is a set of parameters, $\mathcal{Z}_\mathcal{N}$ is the set of observations, $\mathcal{L}$ is the dimension of the observation space, and z_0 is the initial condition. For a given set of parameters and initial states, ϵ_k and $R_{k|k-1}$ are computed by a continuous-discrete extended Kalman filter. The parameter estimates are found by maximising the log-likelihood:

$$\hat{\theta} = \text{argmax}\{\log(L(\theta; \mathcal{Z}_\mathcal{N})|z_0)\}. \tag{15}$$

The corresponding value of the log-likelihood is the observed maximum likelihood value for that data set and model. All computations were done using the free statistical software, R (version 3.3.2), and the "*CTSM-R-package*" (Continuous Time Stochastic Modelling in R version 0.6.8-5, Juhl (2015)).

5. RESULTS

This section describes the results of using the Continuous Time Stochastic Modelling package in R to estimate models for the flow-front. For all model estimates the initial states are assumed to be known. The estimation model does not take the boundary conditions of the PDE into account. Therefore the data used for estimation only include the time steps where all the flow-front progression for all measurement lines are below 0.9 m.

In the homogeneous case the value for the constants in equation (5) are $A = 0.0$ and $c_0 = 3.5 \cdot 10^{-4}$ and for the heterogeneous we have chosen $A = 0.9$ and $c_0 = 1.5 \cdot 10^{-4}$. These have been chosen experimentally to create a flow-front that moves the distance from 0 meter to 0.9 meter to cover the entire area in approximately 600 seconds. For both the homogeneous and the heterogeneous case we perform the model estimation with 5, 8, and 12 line sensor measurements, each at sampling frequencies of 4, 10, and 20 seconds and noise levels with a standard deviation, σ of 0.01, 0.05, and 0.1.

The root-mean-square errors (RMSE) are used to evaluate the estimated models. The resulting RMSE values are calculated as the mean of the RMSE values of the one-step ahead predictions of the states at each time step and these describe how well we estimate our true system. Fig. 5 and Fig. 6 show the relation between the RMSE values and the number of measurement lines, sampling frequency and measurement noise levels for the homogeneous and the heterogeneous cases, respectively. In the homogeneous case the RMSE value is constant w.r.t the number of measurement lines, however generally decreasing with decreasing measurement noise and increasing sampling frequency. For the heterogeneous flow the RMSE is decreasing with increasing number of measurement lines and is in general not affected by changes in measurement noise and sampling frequency. Fig. 7 shows an example of the estimated flow-front trajectories (solid lines) using an estimated flow-front model and the true flow-front trajectories, with measurement noise (dot-dashed), using the PDE model.

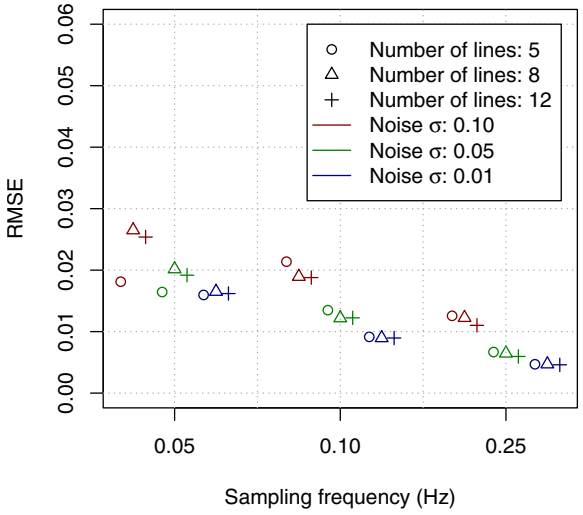

Fig. 5. The RMSE values for the predicted states using models fitted for the homogeneous flow-front data. The data has been perturbed around the specified sampling frequencies for presentation.

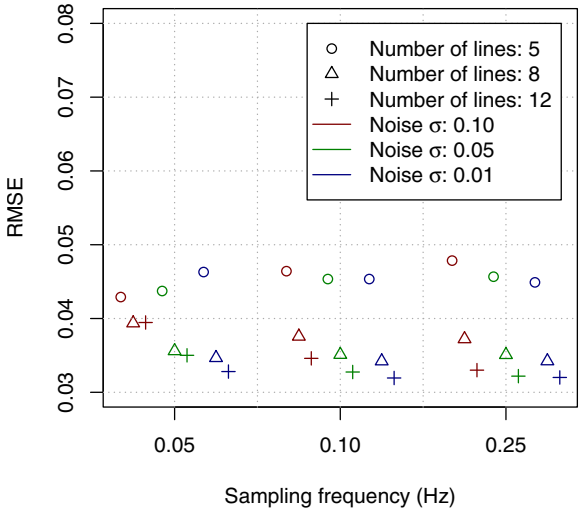

Fig. 6. The RMSE values for the predicted states using models fitted for the heterogeneous flow-front data. The data has been perturbed around the specified sampling frequencies for presentation.

6. CONCLUSIONS AND FUTURE RESEARCH

A good understanding of the flow-front dynamics is essential for designing a monitoring system for controlling the epoxy flow inside the mould in a VARTM process. In this paper, we have proposed a simulation based methodology

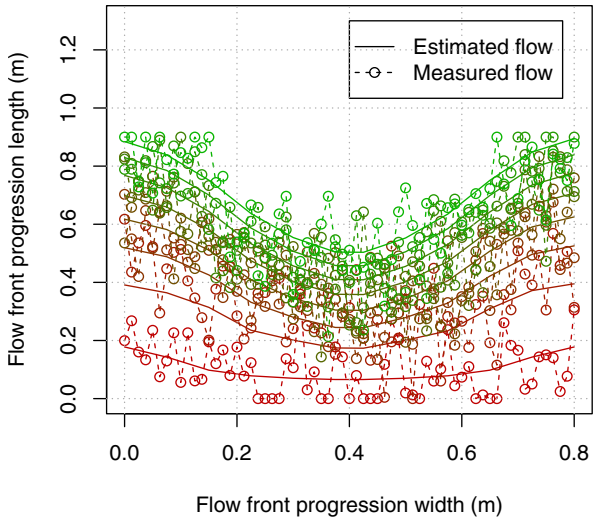

Fig. 7. The estimated flow-front with 12 lines (states), sampling frequency = 0.25 Hz, and the measurement noise $\sigma = 0.1$. The dot-dashed lines indicate the measurements from the true system and the solid lines indicate the estimated flow-front. The line colour changes gradually from red at the first time instance to green at the last time instance.

to understand and model the flow-front dynamics. A PDE based model is proposed to simulate different patterns of the flow-front dynamics for various scenarios. Furthermore, a stochastic differential equations based modelling approach is proposed to estimate a grey-box model of the evolution of the flow-front dynamics inside the mould.

The advantage of coupled SDEs based approach is that it gives the flexibility of combining the partial information about the physics behind the evolution of the flow-front inside mould and the measurements from various sensors (usually pressure or optical sensors in practice) into one parsimonious dynamical model. It can properly handle insufficient knowledge of the system and noise characteristics using the diffusion term in SDEs. The proposed methodology has been validated on simulation examples. The aim of our future research is to test the methodology for more complex flow patterns (e.g. a random change in permeability (w.r.t. displacement), increasing/stochastic viscosity (w.r.t time etc.) and to investigate its validity with real experimental data.

REFERENCES

Alnæs, M.S., Blechta, J., Hake, J., Johansson, A., Kehlet, B., Logg, A., Richardson, C., Ring, J., Rognes, M.E., and Wells, G.N. (2015). The FEniCS project version 1.5. *Archive of Numerical Software*, 3(100). doi:10.11588/ans.2015.100.20553.

Dominauskas, A., Heider, D., and Gillespie, J.W. (2003). Electric time-domain reflectometry sensor for online flow sensing in liquid composite molding processing. *Composites Part A: Applied Science and Manufacturing*, 34(1), 67 – 74. doi:https://doi.org/10.1016/S1359-835X(02)00232-4.

Juhl, R. (2015). *CTSM-R: Continuous Time Stochastic Modelling in R: User's Guide and Reference Manual*. R package version 0.6.8-5.

Kristensen, N.R., Madsen, H., and Jørgensen, S.B. (2004). Parameter estimation in stochastic grey-box models. *Automatica*, 40(2), 225 – 237. doi:https://doi.org/10.1016/j.automatica.2003.10.001.

Kueh, S.R., Parnas, R.S., and Advani, S.G. (2002). A methodology for using long-period gratings and mold-filling simulations to minimize the intrusiveness of flow sensors in liquid composite molding. *Composites Science and Technology*, 62(2), 311 – 327. doi:https://doi.org/10.1016/S0266-3538(01)00217-2.

Matsuzaki, R. and Shiota, M. (2016). Data assimilation through integration of stochastic resin flow simulation with visual observation during vacuum-assisted resin transfer molding: A numerical study. *Composites Part A: Applied Science and Manufacturing*, 84(Supplement C), 43 – 52. doi:https://doi.org/10.1016/j.compositesa.2016.01.006.

Matuzaki, R., Seto, D., Naito, M., Todoroki, A., and Mizutani, Y. (2015). Analytical prediction of void formation in geometrically anisotropic woven fabrics during resin transfer molding. *Composites Science and Technology*, 107(Supplement C), 154 – 161. doi:https://doi.org/10.1016/j.compscitech.2014.12.013.

Nauheimer, M., Relan, R., Madsen, H., Thygesen, U.H., Olesen, B., and Kirkeby, K. (2017). A combined experimental and simulation based approach to model the flow-front dynamics in the vacuum assisted resin transfer moulding process. In *2nd International Conference on Lightweight Design of Materials and Engineering Structures (LIMAS 2017)*, 28–35.

Øksendal, B. (2010). *Stochastic Differential Equations: An Introduction with Applications*. Universitext. Springer Berlin Heidelberg.

Park, C.H., Lebel, A., Saouab, A., Bréard, J., and Lee, W.I. (2011). Modeling and simulation of voids and saturation in liquid composite molding processes. *Composites Part A: Applied Science and Manufacturing*, 42(6), 658 – 668. doi:https://doi.org/10.1016/j.compositesa.2011.02.005.

Sreekumar, P., Joseph, K., Unnikrishnan, G., and Thomas, S. (2007). A comparative study on mechanical properties of sisal-leaf fibre-reinforced polyester composites prepared by resin transfer and compression moulding techniques. *Composites Science and Technology*, 67(3), 453 – 461. doi:https://doi.org/10.1016/j.compscitech.2006.08.025.

Stiesdal, H., Enevoldsen, P., Johansen, K., Kristensen, J., Nörtem, M., and Winther-Jensen, M. (2006). Method for manufacturing windmill blades. EP Patent 1,310,351.

Whitaker, S. (1986). Flow in porous media i: A theoretical derivation of darcy's law. *Transport in Porous Media*, 1(1), 3–25. doi:10.1007/BF01036523.

Yenilmez, B. and Sozer, E.M. (2009). A grid of dielectric sensors to monitor mold filling and resin cure in resin transfer molding. *Composites Part A: Applied Science and Manufacturing*, 40(4), 476 – 489. doi:https://doi.org/10.1016/j.compositesa.2009.01.014.

Zhang, F., Cosson, B., Comas-Cardona, S., and Binetruy, C. (2011). Efficient stochastic simulation approach for rtm process with random fibrous permeability. *Composites Science and Technology*, 71(12), 1478 – 1485. doi:https://doi.org/10.1016/j.compscitech.2011.06.006.